Journal of Materials Chemistry B

Complying the Physiological Functions of Golgi Apparatus for Secretory Exocytosis Facilitated Oral Absorption of Protein Drugs

Journal:	*Journal of Materials Chemistry B*
Manuscript ID	TB-ART-12-2020-002848.R1
Article Type:	Paper
Date Submitted by the Author:	04-Jan-2021
Complete List of Authors:	Xing, Liyun; Sichuan University, Key Laboratory of Drug-Targeting and Drug Delivery System of the Education Ministry and Sichuan Province, Sichuan Engineering Laboratory for Plant-Sourced Drug and Sichuan Research Center for Drug Precision Industrial Technology, West China School of Pharmacy, Sichuan University, Chengdu 610041, China Zheng, Yaxian; West China School of Pharmacy, Sichuan University, Key Laboratory of Drug Targeting and Drug Delivery System Yu, Yinglan; Sichuan University, West China School of Pharmacy Wu, Ruinan; Sichuan University, West China school of pharmacy Liu, Xi; Sichuan University, West China school of pharmacy Zhou, Rui; Sichuan University, Key Laboratory of Drug-Targeting and Drug Delivery System of the Education Ministry and Sichuan Province, Sichuan Engineering Laboratory for Plant-Sourced Drug and Sichuan Research Center for Drug Precision Industrial Technology, West China School of Pharmacy, Sichuan University, Chengdu 610041, China Huang, Yuan; West China School of Pharmacy, Sichuan University, Key Laboratory of Drug-Targeting and Drug Delivery System of the Education Ministry and Sichuan Province, Sichuan Engineering Laboratory for Plant-Sourced Drug and Sichuan Research Center for Drug Precision Industrial Technology, West China School of Pharmacy, Sichuan University, Chengdu 610041, China

Complying the Physiological Functions of Golgi Apparatus for Secretory Exocytosis Facilitated Oral Absorption of Protein Drugs

Liyun Xing, Yaxian Zheng, Yinglan Yu, Ruinan Wu, Xi Liu, Rui Zhou* and Yuan Huang*

Key Laboratory of Drug-Targeting and Drug Delivery System of the Education Ministry and Sichuan Province, Sichuan Engineering Laboratory for Plant-Sourced Drug and Sichuan Research Center for Drug Precision Industrial Technology, West China School of Pharmacy, Sichuan University, Chengdu 610041, China

Abstract

Intestinal epithelial cells are the primary biological barriers for oral administrated nano-formulations and the delivered protein drugs. Thereinto, besides the cellular uptake, intracellular trafficking pathway and the related exocytosis are of great importance to the trans-epithelial transport of drug-loaded NPs. Herein, inspired by the physiological functions of Golgi apparatus for secreting proteins out of cells, Golgi localization related amino acid L-cysteine (Cys) was modified on the surface of NPs to see whether and how this modification could guide the Golgi pathway related transport and facilitate the exocytosis of drug-loaded NPs. Meanwhile, cell-penetrating peptide octa-arginine (R8) was co-modified to increase the cellular uptake. The proportion of R8 and Cys modification was explored to get the best effect of endocytosis and exocytosis of NPs. As a result, 25%R8+75%Cys NPs with most Cys modification showed efficient transcytosis with the highest transcytosis/endocytosis ratio (0.87). Interestingly, exocytosis mechanism studies exhibited that they trafficked through Golgi secretory pathway and bypass lysosomes due to Cys modification. The detailed Golgi position mechanism studies further suggested that the thiol group from Cys was important for mediating Golgi transport. In particular, competitive inhibition studies demonstrated that Cys modified NPs was more conducive to its exocytosis after transported through Golgi secretory pathway. We proved that cargos transported via Golgi apparatus tended to be trafficked out of the cells and avoid degradation, which contributed to the transcytosis of 25%R8+75%Cys NPs *in vitro*. Inspiringly, compared with unmodified NPs, 25%R8+75%Cys NPs also exhibited promoted intestinal penetration and oral absorption *in vivo*. Orally delivery of insulin-loaded 25%R8+75%Cys NPs showed stronger hypoglycemic effect in diabetic rats. In summary, this work

provided a strategy of complying the physiological functions of Golgi apparatus for secreting to facilitate the exocytosis of NPs, thus to further improve the oral absorption of loaded protein drugs.

Keywords: Golgi secretory transport, exocytosis, transcytosis, L-cysteine, nanoparticles, protein drugs, oral absorption

Introduction

Intestinal epithelial cells are the primary biological barriers for nano-formulations to orally deliver protein drugs.[1, 2] Early researches mainly aimed at the enhancement of endocytosis to accelerate trans-epithelial transport of orally administered nanoparticles (NPs).[3-5] Nevertheless, due to the complicated intracellular environments, not all NPs with enhanced cellular uptake showed efficient transcytosis.[6] Most of the NPs would be transported through endolysosomal pathway, which resulted in the degradation of NPs and payloads in the harsh environment of lysosomes.[7] What's more, drug-loaded NPs trapped in cells were difficult to be exocytosed and delivered into blood circulation for systemic effects.[8] Hence, the intracellular NPs urgently deserves a through pathway with mild environment and promoted exocytosis to penetrate the intestinal epithelial cells.

Different from endolysosomal pathway, the secretory pathway, containing Golgi apparatus (Golgi) and endoplasmic reticulum (ER), is considered as a safe approach for drug trafficking.[9-11] Zhang et al. developed ER membrane coated NPs which could transport small interfering RNA (siRNA) through secretory pathway and evade lysosomal degradation, thereby enhanced the effect of siRNA.[12] In secretory pathway, it is worth noting that Golgi apparatus, an organelle of secreting proteins, is closely related to exocytosis. The cargo proteins in Golgi apparatus are modified and destined for secretion to extracellular space via exocytosis.[13, 14] On the basis of the physiological functions of Golgi apparatus, drugs transported via Golgi secretory pathway are expected to be delivered out of the cells.[15] Previous study in our group found that hard NPs tended to be trafficked through Golgi secretory pathway compared with soft NPs, which led to efficient transcytosis through epithelial cells and enhanced oral absorption.[16] Therefore, the Golgi apparatus could be a potential direct train for intracellular NPs to get across the intestinal epithelium.

To our knowledge, the researches on how to deliver cargos to Golgi apparatus in oral delivery systems are still limited. During the development of Golgi probes, ceramide analogues are widely used as Golgi targeting ligand. However, the complex structure, high cost and cytotoxicity limited

their application in orally administration.[17] Inspired by some proteins containing cysteine residues anchored in Golgi apparatus, L-cysteine (Cys) was recently proved to be a Golgi position related amino acid.[18-20] As natural nutrient, Cys has a wide range of sources and good biocompatibility which exhibited great application prospect in oral drug delivery systems.

Herein, Cys was modified on the surface of insulin-loaded NPs (INS NPs) to mediate Golgi localization and subsequent Golgi secretory transport. Cell-penetrating peptide octa-arginine (R8) were additionally decorated on above mentioned NPs to increase the cellular internalization.[21] The proportion of R8 and Cys modification was explored to get the best effect of endocytosis and exocytosis of NPs. In particular, the mechanisms of Golgi localization and Golgi secretory pathway transportation of R8 and Cys co-modified NPs were investigated on Caco-2 cells. Finally, *in vivo* biodistribution and pharmacokinetics of NPs were studied. Also, hypoglycemic effect of orally administered INS NPs was investigated on diabetic rats.

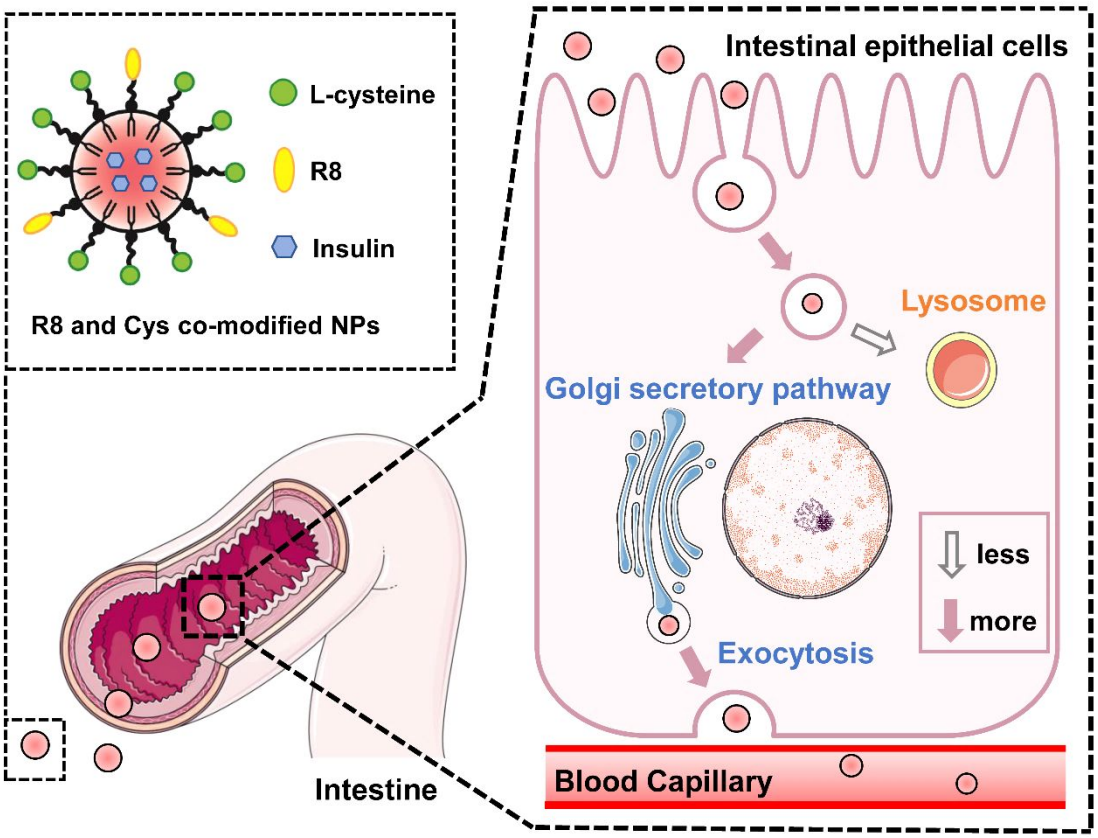

Scheme 1 Schematic illustration of R8 and Cys co-modified NPs through Golgi secretory transport for exocytosis to facilitate intestinal epithelium transportation.

Experimental section

Materials

Poly (lactic-co-glycolic acid) (PLGA, viscosity: 0.26-0.54 dL/g, 50/50) was obtained from Lactel absorbable polymers (Cupertino, CA, USA). DSPE-PEG-NHS (1,2-dioleoyl-*sn*-glycero-3-phosphoethanolamine-*n*-[poly(ethyleneglycol)]-hydroxysuccinimide), DSPE-PEG-Mal (Maleimide) and DSPE-PEG-OMe (Methoxy) (PEG MW: 2000) were provided by Ponsure Biological Co., Ltd (Shanghai, China). Soybean phospholipid was purchased from Taiwei Pharmaceutical Co., Ltd (Shanghai, China). Octa-arginine (R8) peptide with one cysteine end (RRRRRRRRC) was provided by Apeptide Biological Co., Ltd (Shanghai, China). 1,1-dioctadecyl-3,3,3′,3′-tetramethylindocarbocyanine perchlorate (DiI), 3,3- dioctadecyloxacarbocyanine perchlorate (DiO) and 1,1′-dioctadecyl-3,3,3′,3′- tetramethylindotricarbocyanine iodide (DiR) were provided by Invitrogen (Carlsbad, CA, USA). L-cysteine was obtained from Ronggao Biochemical Co., Ltd (Emeishan, Sichuan, China). L-alanine was purchased from Kelong Chemical Co., Ltd (Chengdu, Sichuan, China). Chlorpromazine, simvastatin, amiloride, brefeldin A, chloroquine, alamar Blue, nocodazole, coumarin-6 and monensin were all obtained from Sigma-Aldrich (St Louis, MO, USA). Porcine insulin (28.2 IU/mg) was provided by Wanbang Bio-Chemical Co., Ltd. (Jiangsu, China).

Cells and animals

The human colonic adenocarcinoma (Caco-2) cells were cultured in an incubator (5% CO_2) at 37 °C by using Dulbecco's Modified Eagle's Medium (DMEM, Hyclone, UT, USA) with high glucose which contained 1% (v/v) L-glutamine, 1% (v/v) nonessential amino-acid, 10% (v/v) fetal bovine serum and 1% penicillin and streptomycin (100 IU/mL). Sprague-Dawley (SD) rats (male, 180-220 g), Balb/c mice (male, 18-22 g) and ICR mice (male, 18-22 g) were purchased from Dashuo Biological Technology (Chengdu, China). All experiments were approved by the Institutional Animal Care and Use Committee of Sichuan University.

Synthesis of DSPE-PEG-Cys and DSPE-PEG-R8

L-cysteine (Cys) was conjugated to DSPE-PEG-NHS covalently via ammonolysis of the active ester. Briefly, DSPE-PEG-NHS and Cys were dissolved in phosphate buffer saline (PBS) and mixed (molar ratio of 1:2). Then, the mixture was reacted under stirring at room temperature (r.t) for 24 h and dialyzed in deionized water. DSPE-PEG-Cys was obtained after lyophilization.

Octa-arginine (R8) peptide was covalently conjugated to DSPE-PEG-Mal due to the reaction between maleimide and thiol group. Firstly, R8 and DSPE-PEG-Mal was dissolved in N, N-dimethylformamide (DMF) and mixed in a molar ration of thiol group/maleimide group of 1:1. After stirring at r.t for 24 h, the mixture was dialyzed and lyophilized to afford DSPE-PEG-R8. The structure of obtained conjugates (DSPE-PEG-Cys, DSPE-PEG-R8) were further investigated via ^{1}H NMR spectroscopy.

Preparation and characterization of NPs

Cys or R8 modified nanoparticles were prepared via nanoprecipitation method which was described in our previous work.[22] Unmodified PEG nanoparticles (PEG NPs) were prepared as control by using DSPE-PEG-OMe. Briefly, under stirring conditions (1000 rpm), dimethyl sulfoxide (DMSO) solution (200 μL) containing DSPE-PEG-OMe (0.3 μmol), PLGA (0.2 mg) and soybean phospholipid (0.4 mg) was slowly added into deionized water (4 mL) at r.t to afford the NPs dispersion. In order to prepare NPs modified with different ratio of R8 and Cys, DSPE-PEG-OMe was replaced by different proportion of DSPE-PEG-Cys and DSPE-PEG-R8. The specific content was shown in Table 1. The fluorescent dye DiI, DiO, DiR and coumarin-6 were premixed with the DMSO solution before adding into deionized water to obtain the fluorescent labeled NPs.

Table 1 The amount of DSPE-PEG in the preparation of NPs

Sample	DSPE-PEG-R8 (μmol)	DSPE-PEG-Cys (μmol)	DSPE-PEG-OMe (μmol)
PEG NPs	0	0	0.3
100%Cys NPs	0	0.3	0
25%R8+75%Cys NPs	0.075	0.225	0
50%R8+50%Cys NPs	0.15	0.15	0
75%R8+25%Cys NPs	0.225	0.075	0

NPs modified with different ratio of R8 and Cys was renamed as a%R8+b%Cys NPs (a: molar percentage of DSPE-PEG-R8, b: molar percentage of DSPE-PEG-Cys).

In order to prepare the drug-loaded NPs, certain amount of model drug insulin was further mixed with the above-mentioned DMSO solution. To separate unloaded insulin, the insulin-loaded NPs dispersion was ultrafiltered for 15 min (6000 rpm, 4℃, MWCO of ultrafiltration tube: 100 kDa). Then the total amount of insulin and the amount of unloaded insulin in the supernatant was measured through high performance liquid chromatography (HPLC). The encapsulation efficiency (EE%) and drug loading (DL%) were calculated as follows:

$$EE\% = \frac{\text{Total amount of insulin - unloaded insulin in supernatant}}{\text{Total amount of insulin}} \times 100$$

$$DL\% = \frac{\text{Total amount of insulin - unloaded insulin in supernatant}}{\text{NPs weight}} \times 100$$

Finally, the particle size and zeta potential of obtained NPs were measured via Zetasizer Nano ZS90. The morphology of NPs was observed via transmission electron microscopy (TEM).

Cellular uptake studies

Caco-2 cells were seeded in 96-well plates (1×10^4 cells/well) and cultured for 4 days. The cell number was calibrated by Alamar Blue assay firstly. Then the DiI-labeled NPs (200 μg/mL of

PLGA) were co-incubated with the cells at 37 °C for 3 h. Next, NP suspensions were removed and the iced PBS was applied to wash the cells for three times. Subsequently, DMSO (150 μL) was added into 96-well plate for each hole to destroy the NPs. Finally, the fluorescence intensity of destroyed NPs samples was determined by microplate reader to quantify the internalization of NPs.

Trans-epithelial transport studies

Caco-2 cells were seeded in the transwell (3×10^4 cells/well) and cultured at 37 °C. Then the trans-epithelial electric resistance (TEER) was determined. When TEER value was higher than 800 Ω, the cells could be chosen for the experiment.[23] At first, Hank's Balanced Salt Solution (HBSS) was provided to both apical and basal sides of transwell and incubated for 30 min for equilibration. Then the HBSS in the apical chambers was replaced by DiI-labeled NPs (400 μg/mL of PLGA). At 0, 0.5, 1, 2, 3, 4 and 6 h, medium sample (80 μL) from basolateral chambers was withdrawn into a 96-well plate and HBSS with equal volume was supplemented to the basolateral chamber. Next, 80 μL of DMSO was mixed with the basolateral medium samples. The fluorescence intensity was measured as cellular uptake study described and the apparent permeability coefficient (Papp) value was calculated as following formula:

$$\text{Papp} = \frac{dQ}{dt} \times \frac{1}{\text{A} \times \text{C}_0}$$

Thereinto, dQ/dt is the penetrating rate of DiI-labeled NPs from apical to basal side of transwell, A is the area (cm^2) of transwell membrane, C_0 is the initial concentration of DiI-labeled NPs.

Endocytosis mechanisms studies

Caco-2 cells were seeded and cultured as cellular uptake studies described above. For exploring the endocytosis mechanisms of NPs, the inhibitors of caveolae-mediated endocytosis (simvastatin, 10 μg/mL), micropinocytosis (amiloride, 12 μg/mL) and clathrin-mediated endocytosis (chlorpromazine, 30 μM) were chosen to pre-treated the cells for 30 min. Next, DiI-labeled NPs was added to cells with the presence of corresponding inhibitors and incubated for another 3 h. After removing the solution of NPs and inhibitors, ice-cold PBS were used to wash the cells thrice and DMSO (150 μL) was added into the 96-well plate for each hole. Finally, the fluorescent intensity was determined same as the cellular uptake studies. Uninhibited cells were set as control.

Exocytosis mechanisms studies

Caco-2 cells were cultured as cellular uptake studies mentioned above. For exocytosis mechanism studies, firstly, the cells were treated by DiI-labeled NPs and incubated for 2 h. Next, the NP suspensions were replaced by solutions of different inhibitors which included brefeldin A (25 μg/mL), chloroquine (100 μM), nocodazole (10 μM), monensin (33 μg/mL). 1 h later, the inhibitors were removed from the plate. After washed by iced PBS thrice, DMSO (150 μL) was added to each hole. The fluorescent intensity was measured same as cellular uptake studies mentioned above to quantitively demonstrated the retention of NPs in cells. The cells without treating with inhibitors were set as control.

Subcellular localization of NPs

Caco-2 cells were seeded and cultured in 12-well cell plates which contained coverslips. To study the subcellular colocalization, at first, the cells were incubated with DiO-labeled NPs for 2 h. Next, iced PBS were applied to wash the cells for three times. Then Golgi-Tracker Red (150 μg/mL) and Lyso-Tracker Red (50 nM) were incubated with cells according to the instruction. DAPI were applied to stained the nuclei. Co-localization of NPs and Golgi apparatus or lysosomes was visualized under the confocal laser scanning microscopy (CLSM).

Competitive inhibition of Golgi transport studies

Caco-2 cells were seeded and cultured same as uptake studies mentioned above. For investigating the mechanisms of Cys induced Golgi transport, free Cys was used as competitive inhibitor and free L-alanine (Ala) was selected as negative control. At first, the cells were incubated with DiI- labeled NPs for 2 h at 37℃. Next, the NP suspensions were removed and ice-cold PBS were used to wash the cells thrice. Next, free Cys (100 mM) or free Ala (100 mM) was added. After co-incubation for another 1 h, solutions of Cys and Ala were removed. After washed by iced PBS thrice, DMSO (150 μL) was added to each hole of 96-well plate. the fluorescent intensity was measured to quantitively determine the retention of NPs in cells. The cells not treated with free Cys and free Ala were applied as control.

In situ intestinal penetration studies

Intestinal loop model was applied to investigate *in situ* intestinal penetration of NPs as described previously.[24] Firstly, Sprague-Dawley (SD) rats were anesthetized by chloral hydrate. After mildline laparotomy, 2 cm jejunum loops were selected and the one end was ligated. Next, 200 μL of DiI-labeled NPs were injected into jejunum loops and the other end was ligated. After absorption for 2 h, the jejunum loops were cut out and everted in PBS. After fixed and dehydrated overnight, the jejunum tissues were sliced (thickness: 10 μm). The slices were fixed on a glass slides to prepare the samples. Finally, the samples were observed under CLSM.

Ex vivo intestinal penetration studies

NPs permeated across the jejunum *ex vivo* was quantitatively investigated as described previously.[25] SD rats were firstly anesthetized by chloral hydrate. The jejunum loop sections (2 cm) were cut out and ligated at on end. Next, DiI-labeled NPs (400 μg/mL of PLGA, 200 μL) was injected into the jejunum loops and the other end was ligated. Then the loops were placed into 10 mL Kreb'-Ringer buffer and incubated at 37℃ with continuously aerating by 5% carbon dioxide in oxygen. At 0, 0.5, 1, 1.5, 2, 3 h, the incubation buffer samples (100 μL) were withdrawn into a 96-well plate and Kreb'-Ringer buffer with equal volume was supplemented. The loops were opened at each side, the length and width of loops was measured to calculate the membrane area of jejunum. The fluorescence intensity was determined and the Papp was calculated same as trans-epithelial transport studies above:

$$\text{Papp} = \frac{dQ}{dt} \times \frac{1}{\text{A} \times \text{C}_0}$$

Thereinto, dQ/dt is the penetrating rate of DiI-labeled NPs from jejunum loop to acceptor chambers, A is the area (cm^2) of jejunum loops, C_0 is the initial concentration of DiI-labeled NPs.

Hemolysis assay

At first, blood samples from SD rats were centrifuged (3000 rpm, 5 min). Next, PBS was applied to wash the sediment and the red blood cells (RBCs) were obtained. RBCs was dispersed in PBS with a volume ratio of 1:24. The RBCs were mixed with NPs suspended in PBS (20 μg/mL) in equal volume. Subsequently, the mixtures were incubated for 2 h (60 rpm, 37℃) and centrifuged

for 5 min (1500 rpm). The supernatants were collected and the ultraviolet absorbance (UV-A, 545 nm) was measured. PBS was selected as negative control and 1% Triton was chosen as positive control. Finally, the relative hemolysis efficiency was calculated as follow:

$$\text{Relative hemolysis efficiency\%} = \frac{A_{sample} - A_{PBS}}{A_{1\%\ Triton} - A_{PBS}} \times 100$$

***In vivo* pharmacokinetic and pharmacological studies**

For pharmacokinetic studies, firstly, BALB/c mice were fasted overnight. Coumarin-6-loaded NPs were administered by oral gavage (coumarin-6: 1 mg/kg). Next, blood samples (20 μL) were collected through orbit into a 96-well plate with 80 μL of pure water in each hole. The fluorescence intensity of blood samples was subsequently determined and the pharmacokinetic parameters of coumarin-6 was calculated.[26]

For pharmacological studies, SD rats were intraperitoneal injected with streptozotocin (70 mg/kg) to obtain type I diabetic model rats. After 72 h, the rats (blood glucose level > 16.0 mM) were selected as type I diabetic rats. Saline, INS PEG NPs, INS 25%R8+75%Cys NPs and free insulin solution were administered by oral gavage to three groups of rats separately (insulin: 50 IU/kg) and free insulin solution (insulin: 5 IU/kg) was subcutaneously injected (SC) to another group of rats. At certain time profile, the blood glucose level was measured and the blood samples were collected through the tail veins and at the mean time. Pharmacological availability (PA%) was calculated as follows:

$$PA\% = \frac{(AAC(oral) - AAC(saline)) \times Dose(sc)}{(AAC(sc) - AAC(saline)) \times Dose(oral)} \times 100$$

***In vivo* distribution studies**

For in vivo distribution studies, ICR mice were firstly fasted overnight. Subsequently, DiR-loaded NPs (DiR: 1mg/kg) were orally gavaged to ICR mice. After 4 h, the organs from the mice containing heart, liver, spleen, lung and kidney were harvested. The organs were observed by IVIS Spectrum live imaging system. At last, the fluorescence intensity of liver was determined to quantitative determine the accumulation of DiR-loaded NPs in liver.

Statistical analyses

Student's t-test or one-way analysis of variance (ANOVA) was used for statistical analyses. All data were presented as the mean ± SD. Experiments were performed in triplicate if not specified. Differences at P values < 0.05 were considered to be statistically significant.

Results and discussion

Preparation and characterization of R8 and Cys co-modified NPs

Cys and R8 were conjugated to DSPE-PEG-NHS and DSPE-PEG-Mal via click reaction respectively. The structure of synthesized DSPE-PEG-Cys and DSPE-PEG-R8 conjugates were further investigated via ^{1}H NMR spectroscopy (Fig. S1). The amino groups from Cys could react with NHS and the thiol group at the terminal of R8 could react with maleimide (Mal) group. The feature proton peaks from NHS and Mal group disappeared after reaction, which suggested that Cys and R8 were conjugated to DSPE-PEG-NHS and DSPE-PEG-Mal successfully.

Unmodified PEGylated PLGA NPs (PEG NPs) and Cys modified NPs (100%Cys NPs) were prepared by nano-precipitation technique. In order to further enhance the cellular uptake, R8 was additionally modified on the surface of NPs to develop R8 and Cys co-modified NPs. NPs with specific modification was renamed as a%R8+b%Cys NPs (a: molar percentage of DSPE-PEG-R8, b: molar percentage of DSPE-PEG-Cys). The dynamic light scattering sizes of the NPs were all around 100 nm and the polydispersity index (PDI) was below 0.3 (Fig. 1B). As the amount of positively charged R8 increased, the zeta potential of the nanoparticles also increased from -24.1 mV to -10.8 mV (Fig. 1C). Furthermore, TEM images exhibited the morphology of the NPs (Fig. 1D). Both PEG NPs and NPs with R8 and Cys modification exhibited spherical shape.

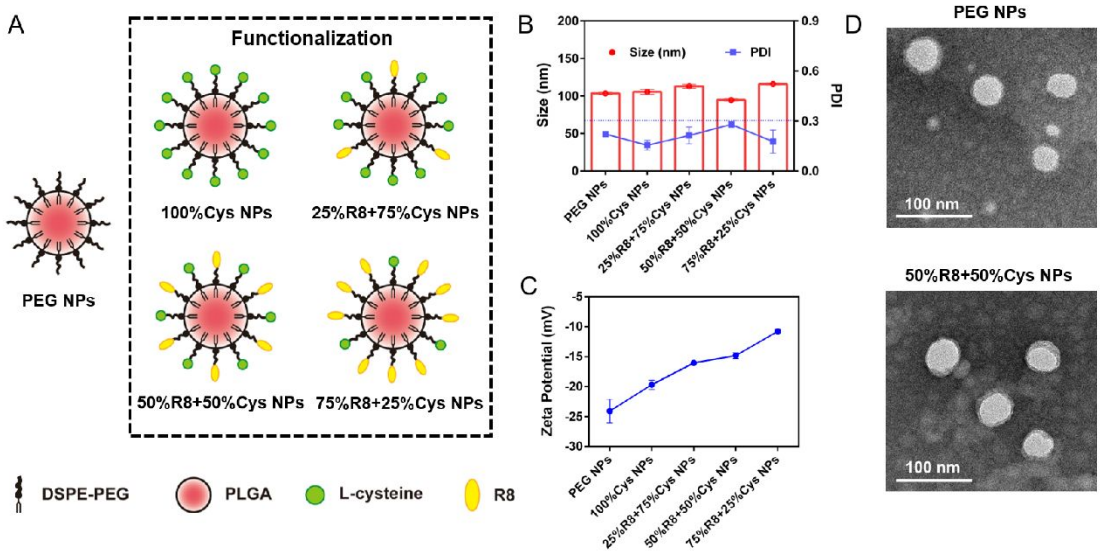

Fig. 1 Characterization of unmodified NPs (PEG NPs) and functionalized NPs (R8 and Cys modified NPs): (A) Illustration of PEG NPs and different ratios of R8 and Cys modified NPs (a%R8+b%Cys NPs, a: molar percentage of DSPE-PEG-R8, b: molar percentage of DSPE-PEG-Cys). (B) Particle sizes and PDI of PEG NPs and R8 and Cys modified NPs. (C) Zeta potential of PEG NPs and R8 and Cys modified NPs. (D) Images of NPs under the observation by transmission electron microscope (TEM), Scale bars: 100 nm.

R8 and Cys modification influenced the endocytosis and transcytosis of NPs

To explore the intestinal epithelial penetration of R8 and Cys modified NPs *in vitro*, both the endocytosis and transcytosis of NPs were investugated on Caco-2 cells. Firstly, all NPs at test concentrations (based on PLGA concentration) demonstrated no cytotoxicity on Caco-2 cells (Fig. S2). Then, compared with PEG NPs, R8 or Cys modification could enhance the internalization of NPs with a concentration dependent manner. (Fig. 2A, 2B). It should be noted that Cys modification demonstrated limited improvement of uptake. R8 modification showed a 2-3 fold higher uptake than the corresponding proportions of Cys, which might be due to the penetrating effect of R8 as well known.[27] Interestingly, additive effects of increased uptake were observed when R8 and Cys were co-modified on NPs. It might be because that Cys could interact with cell membrane via thiol groups in their structure with exofacial thiols which were presented on the surface of cells.[28] 75%R8+25%Cys NPs with most R8 modification showed the highest cellular internalization with 4.75-fold increase than PEG NPs (Fig. 2C). The above results confirmed that both R8 and Cys could increase the internalization of NPs. However, Cys could only slightly affect the cellular uptake, while R8 played a superior role.

Then the effect of R8 and Cys modification on the transcytosis of NPs was investigated (Fig. 2D). The transepithelial electric resistance (TEER) values remained consistent before and after incubation of NPs, which suggested the integrity of cell monolayer during the transcytosis process (Fig. S3). Then the Papp value was calculated to evaluate the trans-epithelial transport rate of NPs (Fig. 2E). In previous studies, the enhanced transcytosis of NPs was usually attributed to their increased uptake.[3-5] However, although the internalization increased along with the R8 modification proportion, 25%R8+75%Cys NPs, 50%R8+50%Cys NPs and 75%R8+25%Cys NPs exhibited nearly the same Papp value (2.27×10^{-6}-2.80×10^{-6}), indicating that the trans-epithelial transport of NPs was not only enhanced by the increased cellular uptake mediated by R8. Cys might also play a vital role in the trans-epithelial transport of NPs.

In order to further explore the role of R8 and Cys played in co-modified NPs, the transcytosis/endocytosis ratio of R8 and Cys co-modified NPs compared with PEG NPs (increased fold of Papp/increased fold of endocytosis) was caculated. As shown in Fig. 2F, although 25%R8+75%Cys NPs with more Cys modification showed relatively weak uptake, it exhibited higher transcytosis/endocytosis ratio (0.87) than 50%R8+50%Cys NPs (0.61) and 75%R8+25%Cys NPs (0.54). Taken collectively, the NPs with more Cys modification might have a stronger tendency to be trafficked out of the cells, which was a benefit for high efficient trans-epithelial transport.

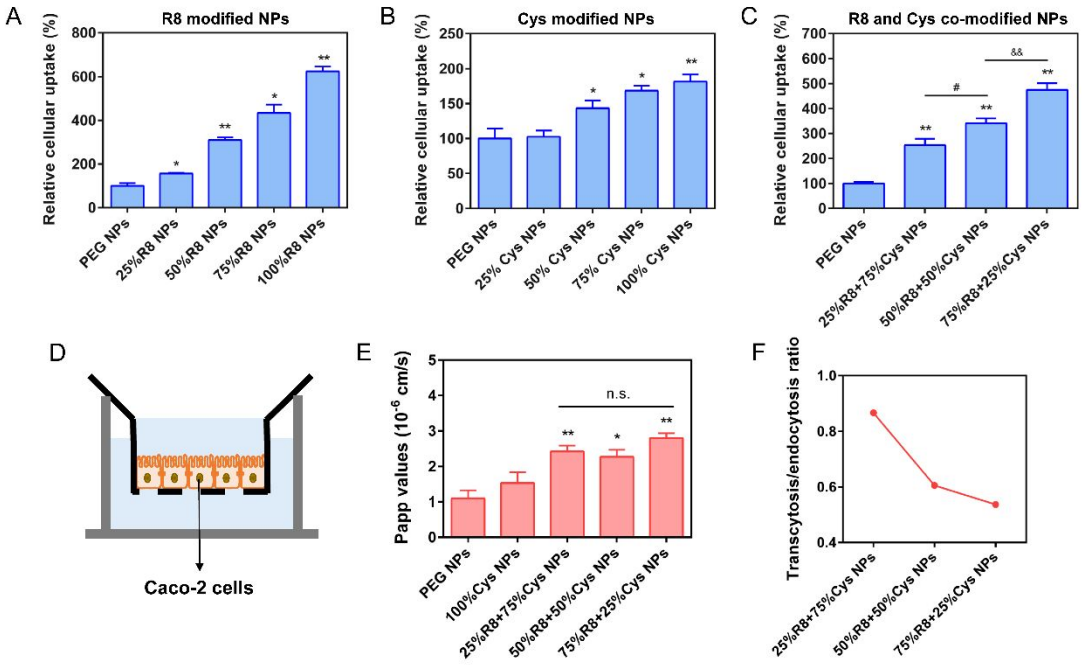

Fig. 2 Endocytosis and transcytosis of NPs. (A) Endocytosis efficiency of R8 modified NPs (n = 3). *P < 0.05, **p < 0.01 compared with PEG NPs. (B) Endocytosis efficiency of Cys modified NPs (n = 3). *p < 0.05, **p < 0.01 compared with PEG NPs. (C) Endocytosis efficiency of R8 and Cys co-modified NPs (n = 3). **p < 0.01 compared with PEG NPs, $^{\#}$P < 0.05 25%R8+75%Cys NPs vs 50%R8+50%Cys NPs, $^{\&\&}$P < 0.01 75%R8+25%Cys NPs vs 50%R8+50%Cys NPs. (D) Transwell chamber model. (E) Papp value of the NPs trafficking through the transwell (n = 3). *p < 0.05, **P < 0.01 compared with PEG NPs. (F) Transcytosis/endocytosis ratio of R8 and Cys co-modified NPs.

R8 and Cys co-modified NPs transcytosed the epithelial cells via Golgi secretory pathway

Next, the transcytosis mechanism of R8 and Cys co-modified NPs was investigated. Three kinds of NPs including 25%R8+75%Cys NPs, 50%R8+50%Cys NPs and 75%R8+25%Cys NPs were chosen for the subsequent study. The cellular uptake of R8 and Cys co-modified NPs was inhibited by chlorpromazine, simvastatin, and amiloride (Fig. 3A), demonstrating the participation of clathrin, caveolae and micropinocytosis mediated endocytosis pathways.[29-31]

The intracellular transport related exocytosis pathway was further studied (Fig. 3B). The inhibitors of endosomal acidification (chloroquine), microtubules (nocodazole), endoplasmic reticulum/Golgi apparatus pathway (brefeldin A) and Golgi apparatus/plasma membrane pathway (monensin) were applied.[32-35] The cellular retentions of the three NPs were all enhanced by brefeldin A, indicating the participation of ER/Golgi trafficking pathway in intracellular transport of the NPs.[36] It was worth noting that with increased amount of Cys modification, the inhibition of the exocytosed NPs by monensin were significantly increased, further suggesting that Cys mediation

may be related to Golgi/plasma membrane pathway. As previously reported, drugs transported in Golgi secretory pathway were proved to be exocytosed from the cells. Since 25%R8+75%Cys NPs had the highest Cys content and transcytosis/endocytosis ratio among three kinds of co-modified NPs, 25%R8 NPs and 75%Cys NPs were prepared to further prove that Cys mediation was related to Golgi/plasma membrane pathway. Interestingly, the exocytosis of 75%Cys NPs was barely inhibited via chloroquine but was significantly reduced by monensin and brefeldin A (Fig. 3C). These results were consistent with the phenomenon that 25%R8+75%Cys NPs were more biased towards the Golgi transport and could avoid lysosomal entrapment, indicating that sufficient modification of Cys could facilitate the transport of NPs through the Golgi secretory pathway. These might be because that Cys modified NPs could be transported to Golgi from plasma membrane or endosomal systems through retrograde pathway.[20] In previous study, such a Golgi related retrograde pathway is not related to the lysosomes.[37, 38] In general, Cys modified NPs could be delivered to Golgi either through the traditional ER/Golgi pathway or through the specific retrograde pathway. Therefore, Cys modified NPs were more tended to be transported through the Golgi and bypass lysosomes. It should be noted that exocytosis of PEG NPs and 25%R8 NPs was significantly inhibited by chloroquine, demonstrating they were trafficked through endolysosomal pathway. According to our previous works, lysosome is considered as a major hinderance during the intracellular trafficking. After endocytosis, most NPs are trafficked into lysosomes via endolysosomal pathway, leading to the retention and degradation of the NPs and payload by acidic environment and hydrolytic enzymes in lysosomes[39]. Golgi apparatus, a major sorting center of the cells, is reported to transport the cargo to cell membrane and extracellular space. Hence, Golgi secretory pathway could be a potential route for transcytosis of oral NPs to access the blood circulation.[6, 15, 37]

To observe the intracellular transport directly, the colocalization of NPs with Golgi apparatus and lysosomes was further observed under confocal laser microscope (CLSM) (Fig. 3D). After staining with Golgi-Tracker Red, the green fluorescence of 75%Cys NPs and 25%R8+75%Cys NPs obviously overlapped with the red fluorescence of Golgi apparatus, showing clear colocalization with Golgi apparatus. Meanwhile, The Pearson's correlation coefficient (Rr) of 75%Cys NPs (0.70) and 25%R8+75%Cys NPs (0.71) which was both higher than PEG NPs (0.59) and 25%R8 NPs (0.58). The results testified the promotion of Golgi transport by Cys. Then, the distribution of NPs

in lysosomes was investigated. PEG NPs and 25%R8 NPs were located in lysosomes obviously (Rr=0.83 for PEG NPs and Rr=0.79 for 25%R8 NPs). 75%Cys NPs and 25%R8+75%Cys NPs exhibited less colocalization with lysosomes. Above all, NPs with Cys modification tended to be trafficked through Golgi secreting pathway and bypassed lysosomes.

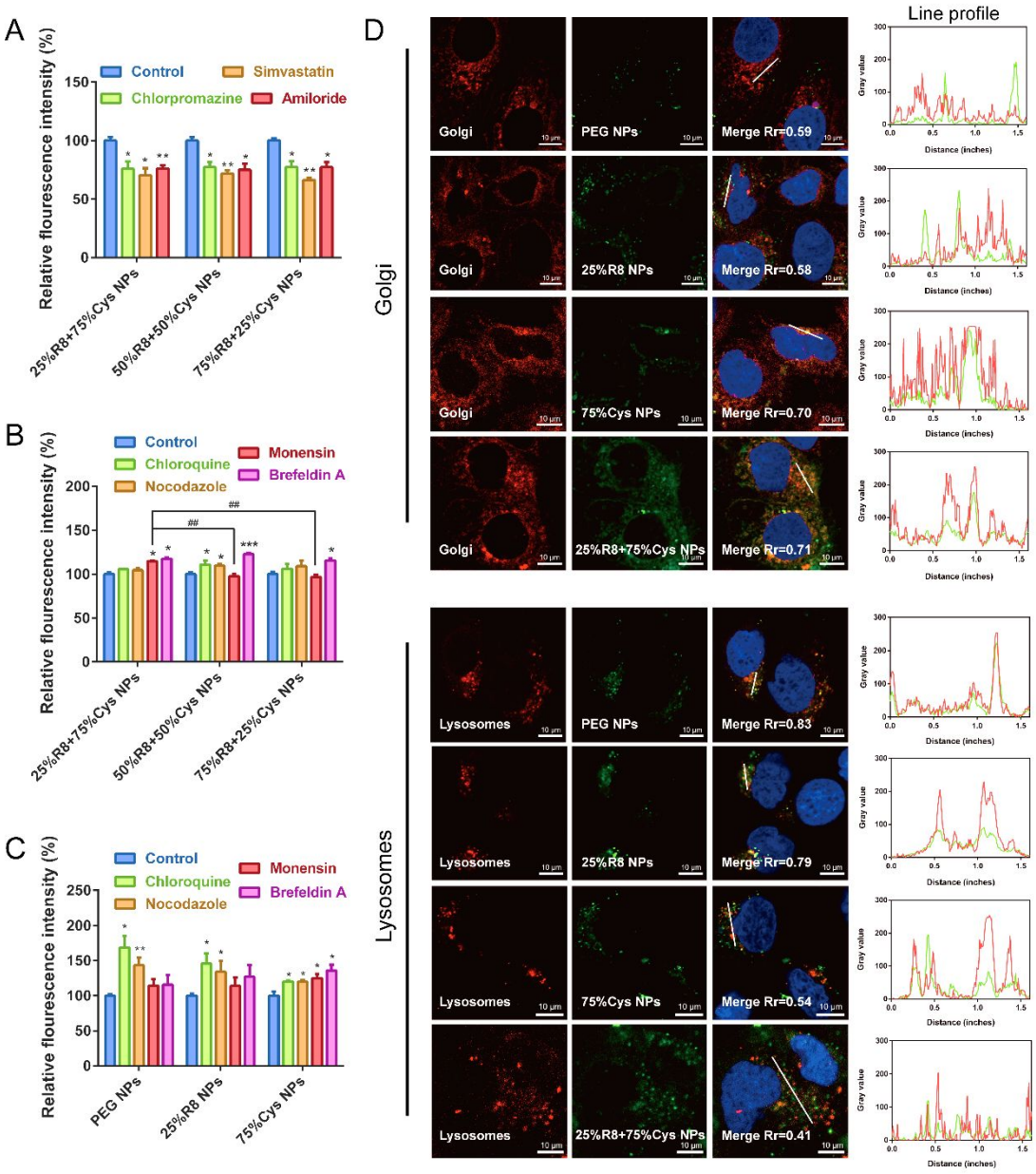

Fig. 3 Endocytosis and exocytosis mechanisms of NPs. (A) Endocytosis mechanisms of R8 and Cys co-modified NPs on Caco-2 cells (n = 3). *P < 0.05, **P < 0.01 compared with control. (B) Exocytosis mechanisms of R8 and Cys co-modified NPs on Caco-2 cells (n = 3). *P < 0.05, ***P < 0.001 compared with control, $^{\#\#}$P < 0.01 25%R8+75%Cys NPs vs 50%R8+50%Cys NPs and 75%R8+25%Cys NPs vs 50%R8+50%Cys NPs. (C) Exocytosis mechanisms of 25%R8 NPs and 75%Cys NPs (n = 3). *P < 0.05, **P < 0.01 as compared with control. (D) Colocalization of NPs with Golgi and lysosomes. Scale bar: 10 μm. Pearson's coefficient (Rr) of NPs colocalized with

Golgi and lysosomes was performed.

Mechanism of cys induced Golgi secretory transport and exocytosis

The results above demonstrated that Cys modification could promote the transport of NPs through Golgi apparatus. Here, the mechanism of Cys promoted Golgi transport for exocytosis was further investigated. Previous studies have found that some proteins such as galactosyltransferase and protein kinase D, etc. could anchored in Golgi apparatus.[18, 19] Thereinto, the cysteine residues in proteins play a great role in localization which might be due to the thiol group of cysteine binding to the sulfhydryl receptor site in Golgi apparatus.[20] Hence, L-alanine (Ala) with the same stereo configuration as Cys but without thiol group was selected as negative control for Golgi colocalization experiment. Ala was connected to DSPE-PEG-NHS and Ala NPs was prepared (Fig. S4). The colocalization of Cys NPs and Ala NPs with Golgi was further observed by CLSM. Among them, Cys NPs was significantly overlapped with Golgi and the Rr was 0.70 (Fig. 4B) which was higher than that of Ala NPs (0.43) (Fig. 4C). This result verified that Cys induced Golgi transport was related to thiol group. Furthermore, Cys induced exocytosis was investigated by competitive inhibition experiment. PEG NPs and Cys NPs were chosen as samples while Cys and Ala were selected as competitive inhibitions (Fig. S5). After internalization of PEG NPs and Cys NPs, free Cys and Ala were separately incubated with the cells. And the results exhibited that the amount of exocytosed PEG NPs was not significantly affected by Cys and Ala. Interestingly, the exocytosis of Cys NPs was not affected by Ala but obviously increased by Cys, suggesting free Cys could promote the exocytosis of Cys NPs (Fig. 4D). This might be because that Cys NPs firstly bind to Golgi through the interaction with sulfhydryl receptor site after uptake, the subsequent incubation of free Cys competed with Cys NPs and led to the secreting of Cys NPs out of Golgi. The NPs were then trafficked to cell membrane and extracellular space for exocytosis. Above all, the thiol group in Cys played a vital role in promoting Golgi secretory transports and related exocytosis.

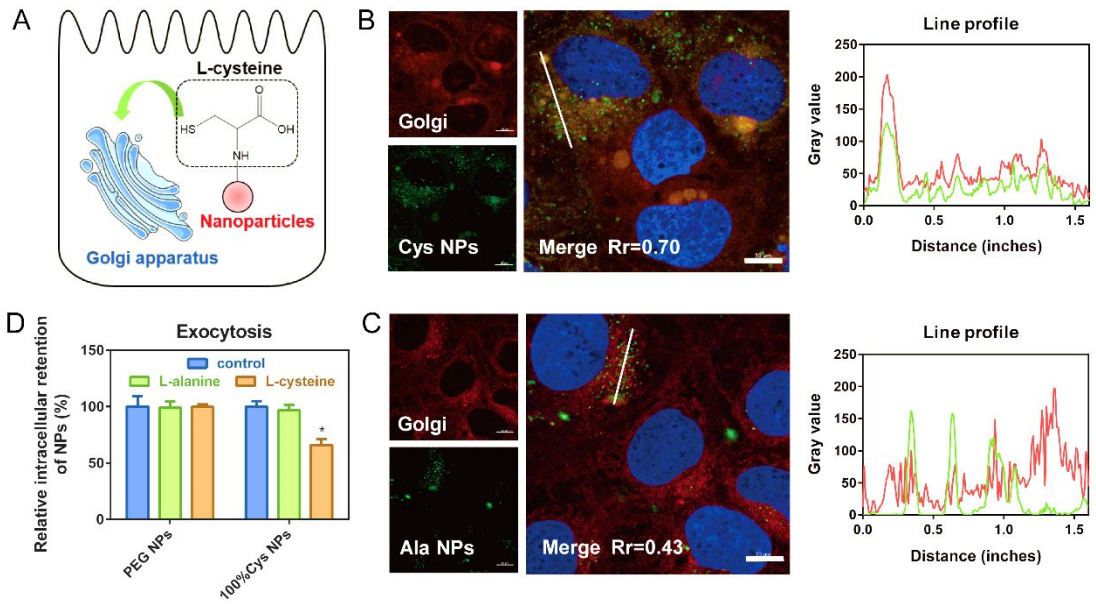

Fig. 4 Mechanism of Cys mediated Golgi transport and exocytosis. (A) Illustration of Cys modification induced Golgi transport. (B) Colocalization of Cys NPs with Golgi. (C) Colocalization of Ala NPs with Golgi. Scale bar: 10 μm. Pearson's coefficient (Rr) of NPs colocalized with Golgi was performed. (D) The intracellular retention of NPs after the additional incubation of free L-cysteine and L-alanine (n = 3). *P < 0.05 vs control.

Golgi secretory transport promoted *in situ* and *ex vivo* intestinal penetration of NPs

To further investigate the correspondence in trends between *in vitro* transcytosis and intestinal mucosa absorption of R8 and Cys co-modified NPs, *in situ* and *ex vivo* ligated intestinal loop models were established. Firstly, the *in situ* absorption of NPs on jejunum of SD rats was observed under CLSM. The distribution of PEG NPs was mainly observed on the apical surface of intestine. After modified with R8 and Cys, more NPs was distributed in the basolateral region of the intestinal villi (Fig. 5B), indicating the enhanced intestinal absorption. The fluorescence intensity of 25%R8+75%Cys NPs, 50%R8+50%Cys NPs and 75%R8+25%Cys NPs was close to each other, suggesting the similar penetration efficiency. Moreover, the *ex vivo* intestinal loop model was applied to quantitively explore the penetration of NPs in intestine. The Papp value of NPs permeated through intestinal loop was calculated (Fig. 5C). 25%R8+75%Cys NPs, 50%R8+50%Cys NPs and 75%R8+25%Cys NPs improved the trans-epithelial absorption to the same extent. The tendency of enhancing *in situ* and *ex vivo* intestinal absorption resembled that of the transcytosis in transwell model. Thereinto, 25%R8+75%Cys NPs showed relatively weak uptake but highest transcytosis/endocytosis ratio, which demonstrated high efficiency of trans-epithelial transport. Based on the mechanism studies above, the promoted Golgi secretory transport might contribute to

intestinal penetration of 25%R8+75%Cys NPs.

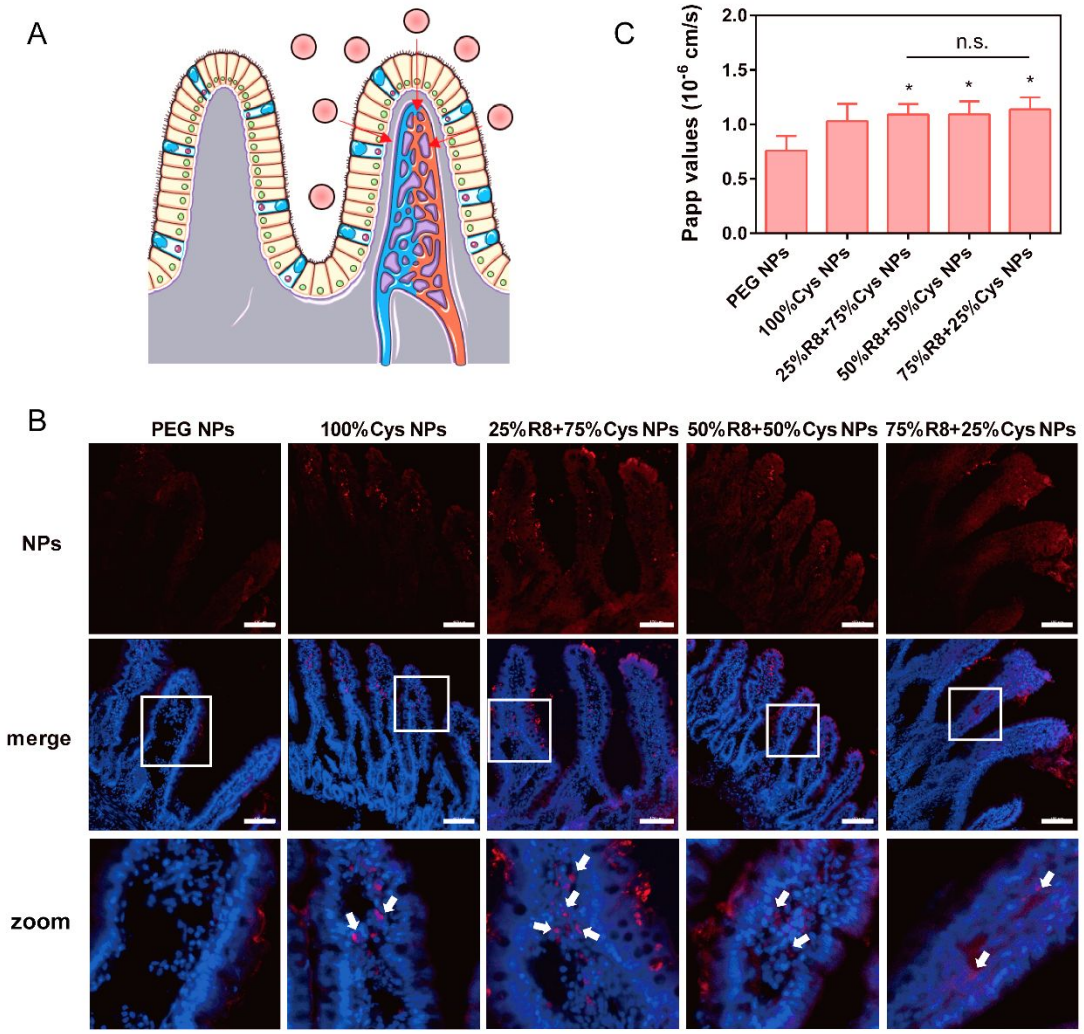

Fig. 5 Intestinal penetration of NPs. (A) Illustration of NPs absorbed by intestinal villi. (B) Images of the intestinal villi in *in situ* intestinal absorption study under CLSM. Blue: nucleus. Red: DiI-labeled NPs. (C) Papp value of NPs penetrating through *ex vivo* jejunum sections (n = 3). *$p < 0.05$ compared with PEG NPs. Scale bar (CLSM): 100 μm.

Golgi secretory transport for exocytosis facilitate oral absorption of NPs

In order to verify the advantage of Golgi secretory pathway on trans-epithelial transport *in vivo*, we investigated the oral absorption of PEG NPs and 25% R8+75% Cys NPs. Both NPs could maintain the stable particle size in simulated gastric fluids (SGF) and simulated intestinal fluids (SIF) (Fig. S6). The hemolysis rate of NPs was lower than 5.0% (Fig. S7), showing good blood compatibility which could be carried out for further oral absorption study. Subsequently, coumarin-6-loaded PEG NPs and 25%R8+75%Cys NPs were administered by oral gavage and the blood concentration of coumarin-6 was measured (Fig. 6A) and the pharmacokinetic parameters were listd

(Table 2). After orally administration, coumarin-6-loaded 25%R8+75%Cys NPs exhibited the faster absorption than PEG NPs. The area under the curve (AUC) was 1.60 fold of PEG NPs. The maximum concentration (C_{max}) of 25%R8+75%Cys NPs was 1.64 times higher than that of PEG NPs. These results demonstrated that NPs trafficking through Golgi secretory pathway was more easily to be absorbed.

Golgi secretory transport improved the hypoglycemic effect of insulin

To further investigate the increased oral absorption of protein drugs-loaded 25%R8+75%Cys NPs for systemic effects, model protein drug insulin (INS) was chosen for orally delivery the and the hypoglycemic effect of various INS formulations on diabetic rats was monitored.[40-42] After loaded with INS, both INS-loaded NPs (INS 25%R8+75%Cys NPs, INS PEG NPs) were around 100 nm. The drug loading efficiency (DL%) of both NPs was around 11% (Table S2). Moreover, due to the protective effect of nanocarriers on peptide/protein drugs, insulin encapsulated in NPs exhibited stronger stability when compared with free insulin under the incubation of trypsin (Fig. S8).

Subsequently, free insulin solution (INS Sol, 50 IU/kg), INS PEG NPs and INS 25%R8+75%Cys NPs (50 IU/kg) were administered to type Ⅰ diabetic rats by oral gavage for hypoglycemic study. Free insulin (5 IU/kg) solution was subcutaneously injected to diabetic rats as positive control and saline was orally administrated as negative control. For the diabetic rats subcutaneously injected with insulin, the blood glucose level was reduced sharply reaching a valley at 2 h, which was 19.38% of initial. Then the blood glucose level was gradually increased to the initial level at 10 h. For orally administration, the diabetic rats remained high blood glucose level in 10 h when orally administered with saline and free insulin solution. These results were in consistence with previous studies, indicating that the rat model was properly built for the assay. In this work, oral INS-loaded NPs exhibited sustained hypoglycemic effect. Thereinto, Oral INS PEG NPs slightly exhibited glucose regulation. By contrast, Oral INS 25%R8+75%Cys NPs significantly reduced blood glucose level to 71.8% of initial in 4 h, which indicated an obviously improved hypoglycemic effect compared with oral administrated insulin solution and INS PEG NPs. Since insulin exerts pharmacological effects in the liver, we investigated the organ distribution of DiR-loaded NPs at 4 h using an *in vivo* imaging instrument (Fig. 6C).[37, 43] Both NPs are mainly distributed

in the liver. The quantitative results showed that the accumulation of 25%R8+75%Cys NPs in liver was significantly more than that of PEG NPs (Fig. 6D), which suggested faster oral absorption of 25%R8+75%Cys NPs. In the end, the pharmacological availability (PA%) of insulin was listed to quantitively determine the hypoglycemic effect of various INS formulations (Table 3). The PA% of INS 25%R8+75%Cys NPs was 3.28 fold of oral INS Sol and 2.56 times higher than INS PEG NPs respectively. These results exhibited the potential of oral absorption and therapeutic effects of INS 25%R8+75%Cys NPs. In general, drug-loaded NPs transported through Golgi secretory pathway for exocytosis were more conducive to the oral absorption of payload and its systemic effects.

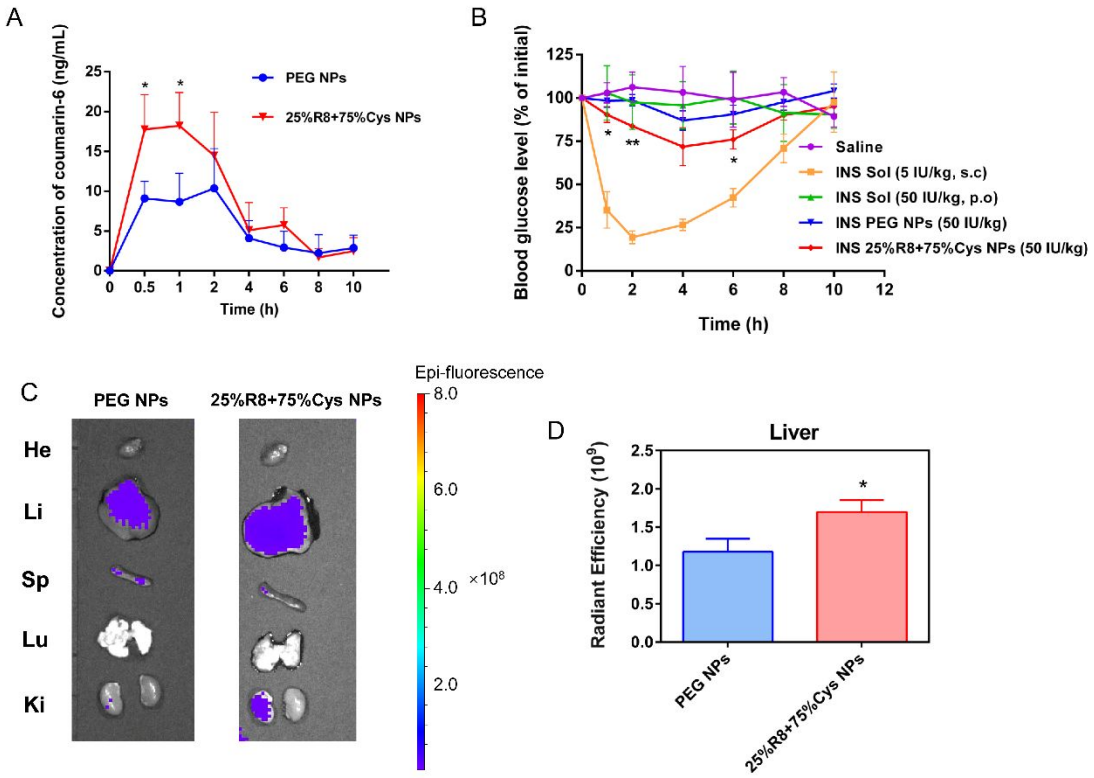

Fig. 6 *In vivo* study. (A) Blood concentration of coumarin-6 after administration of coumarin-6-loaded NPs by oral gavage (n = 5). *P < 0.05 25%R8+75%Cys NPs compared with PEG NPs. (B) After treated with different insulin preparations, blood glucose level vs time profile of type Ⅰ diabetic rats (n = 5). *P < 0.05, **P < 0.01 INS 25%R8+75%Cys NPs vs INS PEG NPs. (C) Images of the biodistribution of DiR-loaded NPs in major organs from mice 4 h after administration by oral gavage. (D) Quantitative determination of DiR in liver via fluorescence intensity (n = 3). *P < 0.05 as compared with PEG NPs.

Table 2 Pharmacokinetic parameters of coumarin-6 in BalB/C mice

Sample	Dose(mg/kg)	C_{max} (ng /mL)	$AUC_{0\text{-}10\ h}$ (ng*h/mL)
PEG NPs	1	11.98±4.60	52.49±16.50
25%R8+75%Cys NPs	1	19.65±4.75	83.95±24.92

Table 3 Pharmacological availability (PA%) of oral insulin in diabetic rats

Sample	INS Sol (i.g)	INS PEG NPs	INS 25%R8+75%Cys NPs
PA(%)	0.93	1.19	3.05

Conclusions

In this research, Golgi apparatus related amino acid Cys was modified on the surface of insulin-loaded NPs. R8 was additionally co-modified to enhance the internalization. As the proportion of Cys increased, NPs demonstrated higher transcytosis/endocytosis ratio and efficient trans-epithelial transport. Interestingly, sufficient Cys modification could promote the transport of NPs through Golgi secretory pathway for exocytosis and bypass lysosomes. Mechanism studies revealed that the thiol group in Cys played a crucial role in mediating Golgi transport. Furthermore, intestinal penetration and *in vivo* absorption studies confirmed that nano-formulations transported via Golgi secretory pathway had advantages in facilitating oral absorption of the payload. What's more, insulin-loaded NPs trafficked through Golgi secretory pathway exhibited stronger hypoglycemic effect. Therefore, Golgi secretory transport conduce to trans-epithelial transport of protein drugs. The strategy of complying the physiological functions of Golgi apparatus showed great application prospect in oral absorption of protein drugs. Our study could provide new inspirations for the development of oral preparations for protein drugs.

Conflicts of interest

The authors declare no competing financial interest.

Acknowledgements

Financial support from the National Science Foundation for Distinguished Young Scholars (81625023), the National Natural Science Foundation of China (81872818) and Youth program of National Natural Science Foundation of China (81903563) are greatly acknowledged.

References

1. M. Duran-Lobato, Z. Niu and M. J. Alonso, *Adv Mater*, 2020, **32**, 1901935.
2. Y. Xiao, Z. Tang, J. Wang, C. Liu, N. Kong, O. C. Farokhzad and W. Tao, *Angew Chem Int Ed Engl*, 2020, **59**, 19787-19795.
3. E. M. Pridgen, F. Alexis, T. T. Kuo, E. Levy-Nissenbaum, R. Karnik, R. S. Blumberg, R. Langer and O. C. Farokhzad, *Sci Transl Med*, 2013, **5**, 213ra167.
4. X. Zhu, J. Wu, W. Shan, W. Tao, L. Zhao, J. M. Lim, M. D'Ortenzio, R. Karnik, Y. Huang, J. Shi and O. C. Farokhzad, *Angew Chem Int Ed Engl*, 2016, **55**, 3309-3312.
5. W. Du, Y. Fan, N. Zheng, B. He, L. Yuan, H. Zhang, X. Wang, J. Wang, X. Zhang and Q. Zhang, *Biomaterials*, 2013, **34**, 794-806.
6. W. Fan, D. Xia, Q. Zhu, L. Hu and Y. Gan, *Drug Discov Today*, 2016, **21**, 856-863.
7. Y. Xu, J. Xu, W. Shan, M. Liu, Y. Cui, L. Li, C. Liu and Y. Huang, *Int J Pharm*, 2016, **500**, 42-53.
8. Y. Cui, W. Shan, R. Zhou, M. Liu, L. Wu, Q. Guo, Y. Zheng, J. Wu and Y. Huang, *Nanoscale*, 2018, **10**, 1494-1507.
9. C. G. Burd, *Traffic*, 2011, **12**, 948-955.
10. M. J. Reilly, J. D. Larsen and M. O. Sullivan, *Molecular pharmaceutics*, 2012, **9**, 1280-1290.
11. N. L. Ross, E. V. Munsell, C. Sabanayagam and M. O. Sullivan, *Molecular therapy. Nucleic acids*, 2015, **4**, 226.
12. C. Qiu, H. H. Han, J. Sun, H. T. Zhang, W. Wei, S. H. Cui, X. Chen, J. C. Wang and Q. Zhang, *Nat Commun*, 2019, **10**, 2702.
13. M. G. Farquhar, *Fed Proc*, 1983, **42**, 2407-2413.
14. F. Bard, L. Casano, A. Mallabiabarrena, E. Wallace, K. Saito, H. Kitayama, G. Guizzunti, Y. Hu, F. Wendler, R. Dasgupta, N. Perrimon and V. Malhotra, *Nature*, 2006, **439**, 604-607.
15. Q. Li, T. Zhou, F. Wu, N. Li, R. Wang, Q. Zhao, Y. M. Ma, J. Q. Zhang and B. L. Ma, *Drug Metab Rev*, 2018, **50**, 430-447.
16. Y. Zheng, L. Xing, L. Chen, R. Zhou, J. Wu, X. Zhu, L. Li, Y. Xiang, R. Wu, L. Zhang and Y. Huang, *Biomaterials*, 2020, **262**, 120323.
17. J. Liu, B. S. Beckman and M. Foroozesh, *Future medicinal chemistry*, 2013, **5**, 1405-1421.
18. Y. Maeda, G. V. Beznoussenko, J. Van Lint, A. A. Mironov and V. Malhotra, *EMBO J*, 2001, **20**, 5982-5990.
19. D. Aoki, N. Lee, N. Yamaguchi, C. Dubois and M. N. Fukuda, *Proc Natl Acad Sci U S A*, 1992, **89**, 4319-4323.
20. R. S. Li, P. F. Gao, H. Z. Zhang, L. L. Zheng, C. M. Li, J. Wang, Y. F. Li, F. Liu, N. Li and C. Z. Huang, *Chem Sci*, 2017, **8**, 6829-6835.

21. S. Jafari, S. Maleki Dizaj and K. Adibkia, *BioImpacts : BI*, 2015, **5**, 103-111.
22. Y. Zheng, J. Wu, W. Shan, L. Wu, R. Zhou, M. Liu, Y. Cui, M. Zhou, Z. Zhang and Y. Huang, *ACS Appl Mater Interfaces*, 2018, **10**, 34039-34049.
23. Y. Bai, R. Zhou, L. Wu, Y. Zheng, X. Liu, R. Wu, X. Li and Y. Huang, *J Mater Chem B*, 2020, **8**, 2636-2649.
24. M. Liu, L. Wu, W. Shan, Y. Cui and Y. Huang, *J Mater Chem B*, 2018, **6**, 593-601.
25. Y. Jin, Y. Song, X. Zhu, D. Zhou, C. Chen, Z. Zhang and Y. Huang, *Biomaterials*, 2012, **33**, 1573-1582.
26. L. Wu, Y. Bai, L. Wang, X. Liu, R. Zhou, L. Li, R. Wu, Z. Zhang, X. Zhu and Y. Huang, *J Control Release*, 2020, **323**, 151-160.
27. E. Koren and V. P. Torchilin, *Trends in molecular medicine*, 2012, **18**, 385-393.
28. A. G. Torres and M. J. Gait, *Trends Biotechnol*, 2012, **30**, 185-190.
29. P. M. Day, D. R. Lowy and J. T. Schiller, *Virology*, 2003, **307**, 1-11.
30. A. I. Ivanov, in *Exocytosis and endocytosis*, Springer, 2008, pp. 15-33.
31. A. Mohan, S. Narayanan, G. Balasubramanian, S. Sethuraman and U. M. Krishnan, *European Journal of Pharmaceutics and Biopharmaceutics*, 2016, **99**, 73-83.
32. C. Homewood, D. Warhurst, W. Peters and V. Baggaley, *Nature*, 1972, **235**, 50-52.
33. G. W. Zieve, D. Turnbull, J. M. Mullins and J. R. McIntosh, *Experimental cell research*, 1980, **126**, 397-405.
34. A. Nebenführ, C. Ritzenthaler and D. G. Robinson, *Plant physiology*, 2002, **130**, 1102-1108.
35. H. H. Mollenhauer, D. J. Morré and L. D. Rowe, *Biochimica et Biophysica Acta (BBA)-Reviews on Biomembranes*, 1990, **1031**, 225-246.
36. R. Y. Yu, L. Xing, P. F. Cui, J. B. Qiao, Y. J. He, X. Chang, T. J. Zhou, Q. R. Jin, H. L. Jiang and Y. Xiao, *Biomater Sci*, 2018, **6**, 2144-2155.
37. A. Wang, W. Fan, T. Yang, S. He, Y. Yang, M. Yu, L. Fan, Q. Zhu, S. Guo, C. Zhu and Y. Gan, *Adv Funct Mater*, 2020, **30**, 1910168.
38. Y. Uchida, J. Hasegawa, D. Chinnapen, T. Inoue, S. Okazaki, R. Kato, S. Wakatsuki, R. Misaki, M. Koike, Y. Uchiyama, S. Iemura, T. Natsume, R. Kuwahara, T. Nakagawa, K. Nishikawa, K. Mukai, E. Miyoshi, N. Taniguchi, D. Sheff, W. I. Lencer, T. Taguchi and H. Arai, *P Natl Acad Sci USA*, 2011, **108**, 15846-15851.
39. Y. Xu, Y. Zheng, L. Wu, X. Zhu, Z. Zhang and Y. Huang, *ACS Appl Mater Interfaces*, 2018, **10**, 9315-9324.
40. S. Shi, N. Kong, C. Feng, A. Shajii, C. Bejgrowicz, W. Tao and O. C. Farokhzad, *Adv Healthc Mater*, 2019, **8**, 1801655.
41. W. Shan, X. Zhu, W. Tao, Y. Cui, M. Liu, L. Wu, L. Li, Y. X. Zheng and Y. Huang, *Acs Appl Mater Inter*, 2016, **8**, 25444-25453.
42. Y. F. Xiao, H. Sung and J. Z. Du, *J Am Chem Soc*, 2017, **139**, 7640-7647.
43. V. T. Samuel and G. I. Shulman, *Cell Metab*, 2018, **27**, 22-41.